JOURNAL OF VIROLOGY, Feb. 1995, p. 871–881
0022-538X/95/$04.00+0

Vol. 69, No. 2

Characterization of the CD48 Gene Demonstrates a Positive Element That Is Specific to Epstein-Barr Virus-Immortalized B-Cell Lines and Contains an Essential NF-κB Site

LORI D. KLAMAN AND DAVID A. THORLEY-LAWSON*

Department of Pathology, Tufts University School of Medicine, Boston, Massachusetts 02111

Received 1 September 1994/Accepted 31 October 1994

Epstein-Barr virus (EBV) infection of mature, resting B cells drives them to become lymphoblasts expressing high levels of cell surface molecules, such as CD48, characteristically expressed on normal activated B cells. Here, we report on the identification of an enhancer element in the CD48 gene which reproducibly confers strong transcriptional activity only in EBV-positive B-lymphoblastoid cell lines. The element is not activated upon infection of established EBV-negative B-cell lines, indicating that EBV fails to drive these cells to a fully lymphoblastoid phenotype. An NF-κB binding site is an essential component of the element but alone is not sufficient to account for the activity or the specificity of the element. We have detected a specific nuclear protein complex that binds to the element and show that NF-κB1 (p50) is a part of this complex. The EBV-encoded latent membrane protein 1 is capable of transactivating the isolated CD48 NF-κB site but not the intact element, suggesting that the latent membrane protein 1-driven activation of NF-κB/Rel must interact with other regulatory pathways to control expression of cellular genes as EBV drives resting B cells into the cell cycle.

Epstein-Barr virus (EBV) is a B-lymphotropic herpesvirus that is associated with several benign and neoplastic diseases in humans (reviewed in references 11 and 29). EBV infects mature, resting B lymphocytes in vitro, causing them to proliferate indefinitely (33), a process that has been termed immortalization or growth transformation. During this process the virus expresses nine proteins, of which six (EBNA-1 to -6) are located in the nucleus and three (latent membrane protein 1 [LMP-1], LMP-2a, and LMP-2b) are located in the membrane. Of these, EBNA-1, -2, -3, and -6 and LMP-1 are essential for growth transformation (19, 20, 39). The immortalized cells do not retain the surface phenotype of resting B cells. Rather, they express elevated levels of B-cell-associated activation antigens and adhesion molecules (7, 21, 36–38, 41, 42). Phenotypically, therefore, they resemble normal B cells that have become activated in response to antigen or mitogens. This observation led to the suggestion that EBV does not directly immortalize B cells but achieves this through two distinct processes (36). The first parallels the normal differentiation pathway for resting B cells whereby they become activated, proliferating lymphoblasts (6, 23, 24). The second involves arresting the cells at this stage, so that they cannot terminally differentiate into plasma cells, resulting in continuous proliferation and the outgrowth of EBV-positive (EBV^+) B-lymphoblastoid cell lines (B-LCLs). It follows that induction of the lymphoblastoid phenotype is an essential step in the mechanism by which EBV immortalizes resting B cells. However, little is known about how EBV regulates cellular gene expression to achieve and maintain this phenotype. Of the cellular molecules known to be induced by EBV, only CD23 has been characterized at the level of transcription (22, 26, 43). Regulatory regions that map to different parts of the gene were identified, but the minimal elements demonstrated weak transactivation (two- to fourfold).

We have chosen CD48 as a model gene to address these issues. The CD48 gene encodes an adhesion molecule (35) that is induced to high levels on the surface of normal, mature, resting B lymphocytes upon infection with EBV. Increased protein expression on the lymphoblast surface is paralleled by a marked increase in CD48 mRNA (45) and remains high on all EBV^+ B-LCLs. The CD48 gene is also constitutively expressed in a wide range of EBV^- lymphoid tumor lines, including Burkitt's lymphomas (BLs). EBV infection of these cells induces only a modest further increase of CD48 mRNA as measured by RNase protection analysis (14). Therefore, it was not possible to map EBV-responsive elements in the CD48 gene by using these cells.

In this study, we used deletion analysis of the upstream region of the CD48 gene to show that this gene is differentially regulated in EBV^+ B-LCLs and EBV^- lymphoid tumor lines. This has allowed us to map an element that confers strong transcriptional activity only in mature normal B cells infected with EBV.

MATERIALS AND METHODS

Plasmid constructions. (i) Serial deletion reporter plasmids. Cloning of the 5′-flanking region of the human CD48 gene and construction of the 1.58-kb *Hin*dIII-*Nsp*I CD48 chloramphenicol acetyltransferase (CAT) construct (−1.58 CAT) has been described previously (13). The CAT construct was digested with *Hin*dIII to remove sequences between −1580 and −234 and religated to obtain deletion construct p−234 CAT. All other deletion constructs were generated from the intact −1.58 CAT reporter gene plasmid by using a Bluescript exo/Mung kit (Stratagene, San Diego, Calif.). Briefly, a *Kpn*I-*Cla*I double digest of −1.58 CAT provided a substrate for the exonuclease III enzyme, which digests in from 5′ overhangs. The shortened plasmids were blunt ended with mung bean nuclease and religated with T4 DNA ligase, resulting in deletion constructs with the following endpoints: −1,442 CAT, −1,245 CAT, −1,066 CAT, −999 CAT, −869 CAT, −599 CAT, −384 CAT, and −110 CAT. All deletion constructs were confirmed by restriction endonuclease analysis and DNA sequencing using the dideoxy-chain termination method (U.S. Biochemical, Cleveland, Ohio).

(ii) Transfection control plasmids. The positive control pCMV/HTLV CAT was obtained from I. S. Y. Chen (5). The negative control pSL1 CAT was

* Corresponding author. Mailing address: Department of Pathology, Tufts University School of Medicine, 136 Harrison Ave., Boston, MA 02111. Phone: (617) 636-4726. Fax: (617) 636-8590.

described previously (13). The cotransfected internal control construct pCMV β-galactosidase was obtained from G. MacGregor (Baylor University, Tex.). The LMP-1 expression vector pSV2 BNLF1 (2) was kindly provided by Bill Sugden. The mutant construct mt NFκB TK (thymidine kinase) contains two copies of a mutated upstream regulatory element (URE) NF-κB site from the murine c-*myc* gene (10). The pCD48 NFκB TK CAT construct was prepared by digesting the URE TK CAT construct with *Bam*HI, which should drop out the URE sequences, and inserting two copies of the CD48 NF-κB site (5′-GATCCTTTCA TAAGGAAGGGGCTTTCCCCATTGG-3′). The site, with terminal *Bam*HI sites for cloning, and its complementary sequence were synthesized on an automated DNA synthesizer (Applied Biosystems). The mutant and wild-type URE TK CAT constructs (10) were generously supplied by Gail Sonenshein.

(iii) Preparation of enhancer constructs. Serial deletion construct −1,066 CAT was digested with *Bam*HI, which opens the plasmid in the polylinker region of the Bluescript KS+ plasmid, 3′ of the bacterial CAT gene. A PCR-amplified product, corresponding to human CD48 upstream sequences from −1245 to −1066, was engineered with *Bam*HI ends and subcloned into the *Bam*HI-digested −1,066 CAT vector. Enhancer plasmids were checked by dideoxy sequencing to eliminate PCR-derived errors and to determine the sense or antisense orientation of the insert. All plasmid DNA used for transfections was purified with Qiagen maxicolumns (Qiagen, Studio City, Calif.).

Oligonucleotides. A 34-bp oligonucleotide containing the human immunoglobulin kappa (Igκ) light-chain NF-κB consensus sequence (5′-ATTCCCCCAG AGGGGGATTTCCAAGAGGCCACCT-3′) and a corresponding oligonucleotide with a mutated human Igκ light-chain NF-κB consensus sequence (5′-ATTCCCCCAGAGGCGGATTTCGAAGAGGCCACCT-3′) were synthesized with their complementary sequences on an automated DNA synthesizer (Applied Biosystems) and annealed. A double-stranded oligonucleotide containing the mouse Igκ light-chain NF-κB consensus site was purchased from Promega (Madison, Wis.). Double-stranded oligonucleotides containing the EBNA-1 and Oct-1 binding sites were purchased from Pharmacia (Piscataway, N.J.). Annealed oligonucleotides were end labeled with γ-^{32}P-labeled deoxynucleoside triphosphates and purified over a NucTrap column (Stratagene).

Site-directed mutagenesis. Mutant CAT reporter plasmids were made with the Amersham oligonucleotide-directed in vitro mutagenesis system (Amersham, Arlington Heights, Ill.), with some modifications. The Bluescript phagemid (Stratagene) with the −1.58 CAT sequences was used in place of recombinant M13 as the single-stranded DNA template. −1.58 CAT single-stranded DNA was rescued with the R408 helper phage by using a protocol supplied by Stratagene. To introduce mutations into the NF-κB site (−1149 to −1133), the oligonucleotides mutant 1 (mt1; 5′-GGTTTCATAAGGAAGCGGCTTTGCC CATTGCTGCTCAG-3′) and mt2 (5′-GGTTTCATAAGGAATGGTCTTGCG CCATTGCTGCTCAG-3′) were designed with consideration to the reported frequency of base usage at each position of the consensus NF-κB site (17).

Cell culture. The EBV$^+$ B-LCL X50-7 and the EBV$^-$ BL cell line DG75 were kind gifts of Sam Speck (Washington University, St. Louis, Mo.). The EBV$^+$ B-LCL IB4 was kindly provided by Elliot Kieff (Harvard University Medical School, Boston, Mass.). The EBV$^+$ B-LCL JY was previously established in our laboratory. The EBV$^-$ BJAB line, the BL41 BL line, and their EBV-converted counterparts BJAB B95-8 and BL41 B95-8 were a generous gift of Gilbert Lenoir (Lyon, France). The helper T-cell line Jurkat, the erythroleukemic cell line K562, and the fibroblast line HEL299 were obtained from the American Type Culture Collection (Rockville, Md.). All cell lines were cultured in RPMI 1640 medium supplemented with 10% fetal bovine serum, 100 U of penicillin per ml, and 50 μg of streptomycin per ml. Nuclear extracts were prepared by a modification of the Dignam method (1). Several preparations of extract were isolated and tested for binding activity with the ubiquitous Oct-1 binding site as a positive control. The protein concentration of the nuclear extract was assayed by the Bradford method (Bio-Rad, Hercules, Calif.). Extracts were stored at −70°C.

Transfection of cell lines. With the exception of HEL299, all cell lines were transiently transfected by electroporation. Transfections of HEL299 cells were performed by the $CaCl_2$ method (16). For each electroporation, 2×10^7 cells were washed once in phosphate-buffered saline, resuspended in 0.5 ml of Gibco Optimem, and transferred to a Bio-Rad Gene Pulser cuvette containing 20 μg of CAT reporter gene construct DNA and 5 μg of pCMV β-galactosidase DNA, an internal control plasmid included to monitor transfection efficiency. For cotransfection experiments, 10 μg of reporter construct was mixed with 10 μg of the cotransfected expression vector. Cells and DNA were mixed gently, and the cuvette was placed on ice for 10 min immediately preceding and following electroporation in a Bio-Rad Gene Pulser. Optimal transfection conditions for each cell line were determined by using the positive control pCMV/HTLV CAT.

Analysis of transfected cells. Cell lysates were harvested 48 h posttransfection, resuspended in 250 mM Tris-HCl (pH 7.5), and subjected to three freeze-thaw cycles with liquid N_2. Cell lysates, normalized for protein concentration (Bradford dye reagent kit; Bio-Rad), were used to assay transfection efficiencies in a β-galactosidase assay (34). For individual CAT assays, equal β-galactosidase units were incubated in a total volume of 150 μl containing 250 mM Tris-HCl (pH 7.5), 68 μM acetyl coenzyme A, and 0.05 μCi of [^{14}C]chloramphenicol for 2 h at 37°C. CAT activity was assayed by the standard method of Gorman et al. (15). Acetylated and nonacetylated [^{14}C]chloramphenicol activity was quantitated by analyzing the thin-layer chromatographic plates following exposure to PhosphorImager screens (Molecular Dynamics, Sunnyvale, Calif.).

EMSA. For protein-DNA binding reactions, 5 μg of nuclear extract was mixed with 1.5 μg poly(dI-dC) in a total volume of 20 μl consisting of 10 mM Tris-HCl (pH 7.5), 50 mM NaCl, 10% glycerol, 0.05% Nonidet P-40, 5 mM $MgCl_2$, 0.5 mM dithiothreitol, and 0.5 mM phenylmethylsulfonyl fluoride. Following the addition of 1.0 ng of α-^{32}P-end-labeled DNA probe (~20,000 cpm), the reaction mixtures were incubated for 20 min at 25°C. Where indicated, a 25- to 200-fold molar excess of unlabeled competitor DNA or unrelated DNA was added 10 min prior to the addition of the labeled probe. The reaction products were resolved on 5% nondenaturing polyacrylamide gels (40:1 cross-linking ratio; in 0.5× Tris-glycine at 4°C). For supershifting electrophoretic mobility shift assays (EMSAs), binding reaction mixtures were incubated with 1 μl (per 5 μg of nuclear extract) of the appropriate antisera, or a preimmune control, for 20 min at 4°C prior to the addition of the end-labeled probe. NF-κB1 (p50), RelA (p65), and c-*rel* supershifting antisera were generously supplied by Nancy Rice (Frederick, Md.) and Uli Siebenlist (National Institutes of Health, Bethesda, Md.).

DNase I footprinting. For DNase I protection assays, α-^{32}P-end-labeled probes were incubated with nuclear extract in a reaction mixture that had been scaled up fivefold from the EMSA binding reaction. The mixture was digested with 10 μg of DNase I per ml for 2 min at 25°C. Equal counts per minute of bound and free samples were resolved on an 8% polyacrylamide–8 M urea sequencing gel. Footprint data were obtained on both strands and the positions of the protected regions were determined by reference to a G+A Maxam-Gilbert ladder (28) resolved in parallel.

RESULTS

CD48 5′-flanking sequences that regulate responsiveness in EBV$^+$ B-LCLs. A CAT reporter gene construct (−1.58 CAT) containing 1.58 kb of sequences 5′ of the transcriptional start sites of the CD48 gene has been described previously (13). A series of 5′ deletions were derived from −1.58 CAT, and their structures are shown in Fig. 1. These constructs were transiently transfected into a panel of EBV$^+$ and EBV$^-$ cell lines (Table 1) to localize transcriptional elements that regulate expression of the CD48 gene. Relative activities of the deletion constructs are displayed (Fig. 1) for IB4 and BJAB, representative of EBV$^+$ B-LCLs and EBV$^-$ lymphoid cell lines, respectively. Data for the most important constructs (−1.58 CAT and −869 CAT) are presented, for all cell lines tested, in Fig. 2.

The largest deletion with consistently high reporter gene activity was −234 CAT. This construct had promoter activity that reflected the behavior of the endogenous CD48 gene. It was active in B- and T-cell lines irrespective of EBV status (e.g., Fig. 1) but not in nonlymphoid lines (not shown), suggesting the presence of a lymphoid cell-restricted proximal element. Constructs with smaller deletions showed progressively weaker activity until −869 CAT, which displayed only basal levels of activity in all cell lines (Fig. 2). In the case of the EBV$^-$ cell lines, the trend continued such that the activity of the undeleted −1.58 CAT in these cells was indistinguishable from the activity of the negative control (pSL1 CAT) construct. However, in the case of the EBV$^+$ B-LCLs, the trend was dramatically reversed such that the activity of −1.58 CAT was even higher than that obtained with −234 CAT (Fig. 1B). Within a given experiment, activations of 15- to 75-fold were seen when we compared −1.58 CAT and −869 CAT in the

TABLE 1. EBV$^+$ and EBV$^-$ cell lines used

EBV status	Cell line	Cell type
+	IB4	B lymphoblast
	JY	B lymphoblast
	X50-7	B lymphoblast
−	DG75	B lymphoma (Burkitt)
	BL41	B lymphoma (Burkitt)
	BJAB	B lymphoma
	Jurkat	T leukemia
	K562	Erythroleukemia
	HEL299	Fibroblast

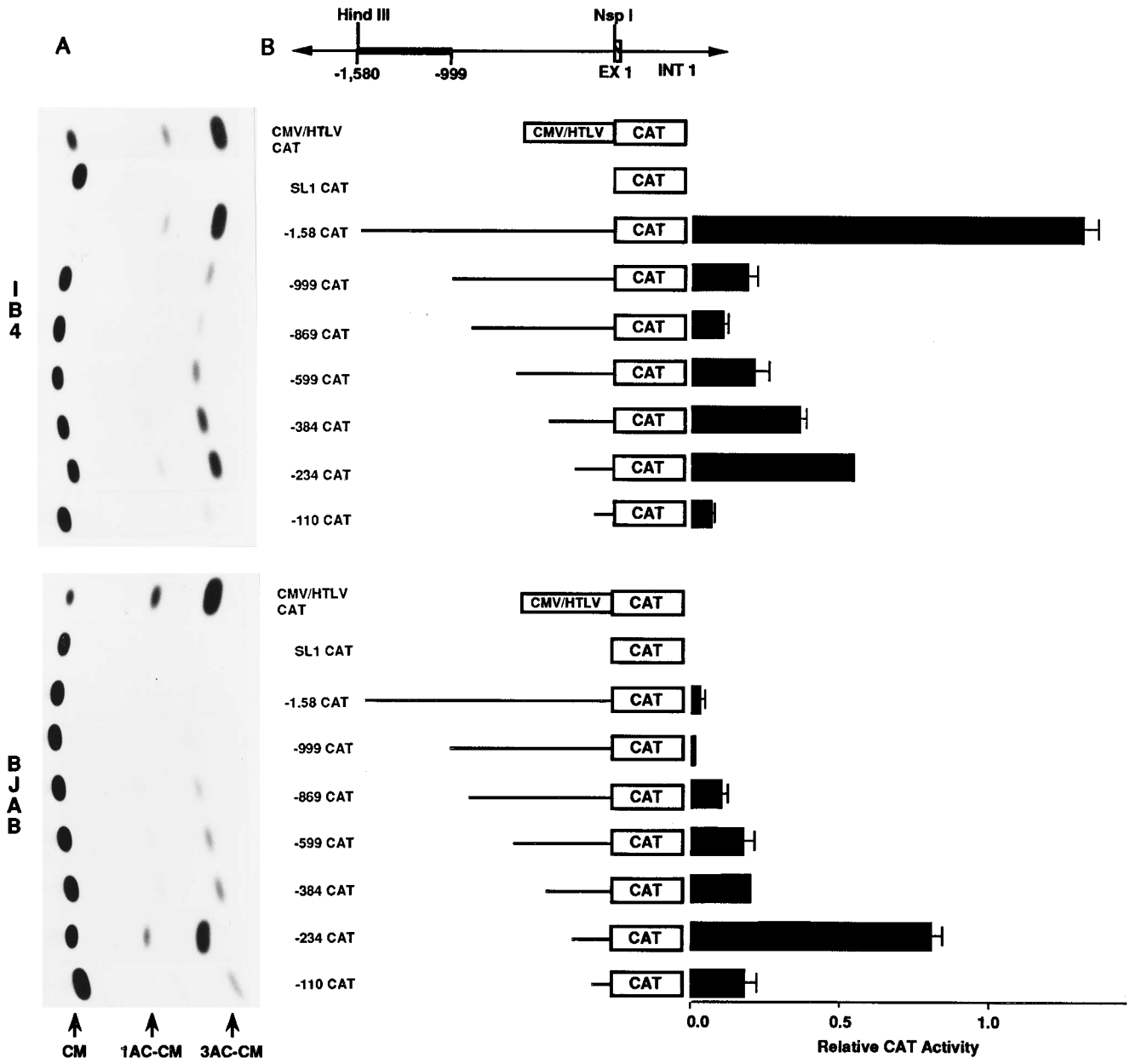

FIG. 1. Mapping of the EBV-responsive element. Regulatory sequences within the *Hin*dIII-*Nsp*I CD48 genomic fragment were mapped by measuring the transcriptional activity of −1.58 CAT and deletion plasmids, using various lengths of the 5′-flanking region to drive transcription of CAT. (A) Transient transfection results for an EBV$^+$ and EBV$^-$ cell lines, IB4 and BJAB, respectively. A total of three independent transfection experiments were performed in duplicate for each cell line, with a representative assay shown. Acetylated (1AC-CM and 3AC-CM) and unacetylated (CM) forms of [^{14}C]chloramphenicol are indicated by arrows at the bottom. (B) Structure of the *Hin*dIII-*Nsp*I CD48 genomic DNA fragment. The thick bar indicating the region which contains the EBV-responsive element as defined by crude deletion mapping of CD48 CAT plasmids. Ex 1, exon 1; INT 1, intron 1. A schematic view of the 5′-flanking sequence is shown for each CAT construct, including the positive control and negative control plasmids, pCMV/HTLV CAT and pSL1 CAT, respectively. pCMV/HTLV CAT activity is assigned an arbitrary value of 1.0. The bar graph shows quantitation of relative CAT activity following transfection of −1.58 CAT or CD48 deletion constructs into IB4 and BJAB.

same EBV$^+$ B-LCL or compared −1.58 CAT between an EBV$^+$ B-LCL and an EBV$^-$ cell line.

These experiments demonstrate that the CD48 promoter is negatively regulated in lymphoid cell lines, by elements located between positions −234 and −869. These silencers can be overcome by an element that lies further upstream (between −1580 and −999). Because this element specifically functions only in EBV$^+$ B-LCLs, we refer to it as EBV responsive. Since the endogenous CD48 gene is also active in EBV$^-$ lymphoid tumor lines but −1.58 CAT is not, there must be additional positive elements, not present in this construct, to account for CD48 gene expression in the EBV$^-$ lymphoid tumor lines.

The CD48 EBV-responsive element is an enhancer. We constructed a finer set of deletion mutants between −1.58 CAT and −869 CAT to more precisely map the boundaries of the EBV-responsive element. The CAT assay for this set of deletion mutants is shown for IB4 (Fig. 3A) and is representative of all EBV$^+$ B-LCLs (not shown). Deletion constructs up to −1,245 CAT demonstrated activity similar to that of −1.58 CAT, but the next deletion, −1,066 CAT, and subsequent

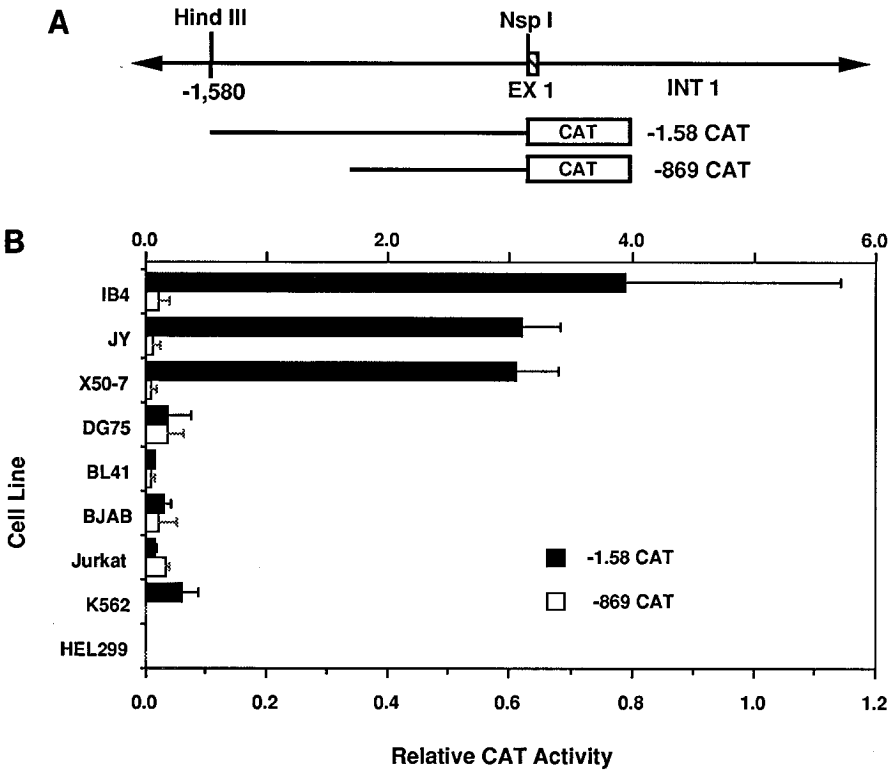

FIG. 2. Demonstration of an EBV-responsive element. (A) Structure of the *Hin*dIII-*Nsp*I CD48 genomic DNA fragment, extending 1,580 bp upstream of the translational start site of exon 1 (EX 1), used to construct −1.58 CAT. INT 1, intron 1. (B) Quantitative comparison of relative CAT activities following transient transfection of −1.58 CAT or deletion construct −869 CAT into EBV^+ B-LCLs and EBV^- cell lines (see Table 1). The percentage of [^{14}C]chloramphenicol conversion is reported relative to that of the positive control construct pCMV/HTLV CAT, which is assigned an arbitrary value of 1.0. Upper axis, scale for IB4; lower axis, scale for all other cell lines. Reported values represent the means and standard deviations from three independent experiments each in duplicate.

deletions displayed a ≥10-fold drop in CAT activity and were indistinguishable from −869 CAT. None of the deletion mutants in this set displayed detectable CAT activity in the EBV^- cell lines (not shown). This experiment localized the EBV-responsive element between positions −1245 and −1066.

Next, we tested this region for enhancer activity by inserting the missing EBV-responsive sequences at the 3′ end of the CAT gene in the inactive deletion plasmid −1,066 CAT. As shown for IB4 (Fig. 3B), reintroducing these sequences, in either the sense or antisense orientation, fully restored transcriptional activity in EBV^+ B-LCLs to levels as high as those seen with deletion construct −1,245 CAT. This result demonstrates that the EBV-responsive element(s) behaves in an orientation- and position-independent manner, two features which classically define an enhancer.

DNase I footprinting of the EBV-responsive element. We performed DNase I footprinting analysis with EBV^+ B-LCL and EBV^- nuclear protein extracts to identify nucleotide sequences that could mediate EBV responsiveness of the CD48 gene. A specific footprint was obtained (Fig. 4A, lanes 2 to 5) when a labeled DNA probe spanning positions −1181 to −1053 was incubated with nuclear extracts isolated from the IB4 B-LCL. Neither BJAB nor K562 nuclear proteins protected this probe from DNase I digestion even at the highest concentration of extract tested (Fig. 4A, lanes 6 to 11). The same footprint was obtained with nuclear extracts from JY but not with extracts prepared from DG75 (not shown). The protected nucleotide sequence, 5′-GGAAGGGGCTTTCCCCA-3′, was localized between positions −1149 and −1133. EBV^+ nuclear extracts displayed a similar footprint on the complementary strand (Fig. 4B). Comparison with known binding sites for nuclear proteins (12, 17) revealed homology of the core protected region (GGGGCTTTCC) to a consensus binding site for the NF-κB/Rel family of transcription factors.

Mutational analysis of the putative NF-κB site. We mutated nucleotides in the putative NF-κB motif to determine whether this site is an essential component of the EBV-responsive element. Nucleotide substitutions that would ablate an NF-κB site as judged from previously published analyses (3, 17) were chosen. Wild-type and mutated DNA fragments spanning positions −1181 to −1053 were subjected to DNase I footprinting in the presence of nuclear extracts prepared from the EBV^+ B-LCL IB4. Lane 6 to 9 of Fig. 5A display the footprinting pattern for mt1, a probe which contains nucleotide substitutions at positions 2 and 9 of the NF-κB consensus site. A protected footprint was no longer evident compared with the wild-type pattern (lanes 2 to 5), even in the presence of increasing amounts of nuclear extract. The same result was obtained with mt2, which contains four nucleotide substitutions in the NF-κB consensus sequence at positions 1, 4, 8, and 10 (not shown).

Mutated −1.58 CAT plasmids were generated with the same base substitutions described above for mt1 and mt2. The relative CAT activities of the wild-type and mutated −1.58 CAT plasmids were then compared to determine whether the putative NF-κB site was required for the activity of the EBV-responsive element. As shown for IB4 (Fig. 5B), the mutated −1.58 CAT plasmids were not able to stimulate CAT activity following transfection into the EBV^+ B-LCLs, while the positive control pCMV/HTLV CAT and wild-type −1.58 CAT

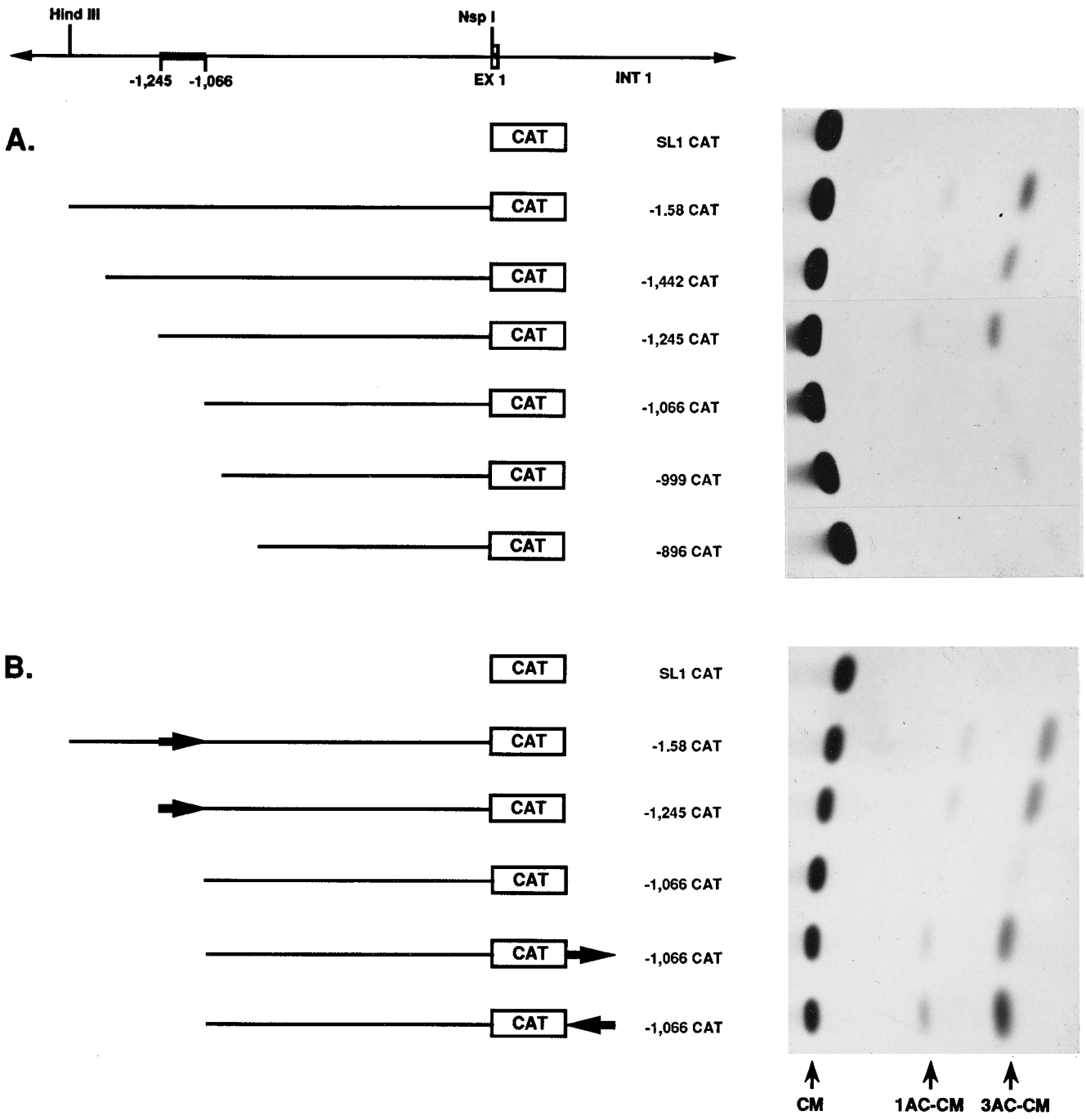

FIG. 3. Fine deletion mapping localizes an EBV-responsive enhancer element. The structure of the CD48 genomic DNA fragment is shown. EX 1, exon 1; INT 1, intron 1. (A) A finer series of 5′-deletion constructs were generated between −1.58 CAT and −869 CAT and tested for transcriptional activity in EBV$^+$ B-LCLs (results shown for IB4). The location of the EBV-responsive element, as defined by fine deletion mapping, is indicated by the thick bar above. (B) CD48 enhancer constructs were derived by subcloning the EBV-responsive element (bold arrows) into plasmid −1,066 CAT at the 3′ end of the bacterial CAT reporter gene in either the sense (→) or antisense (←) orientation. −1.58 CAT and the CD48 enhancer constructs were tested for transcriptional activity in EBV$^+$ B-LCLs as described in the legend to Fig. 1 (results shown for IB4).

plasmids demonstrated high levels of activity. Similar results were obtained following transfection of the mutated plasmids into JY (not shown). Thus, mutagenesis of the putative NF-κB site resulted in concomitant loss of the specific DNase I footprint and detectable enhancer activity. We conclude, therefore, that the putative NF-κB site is an essential component of the EBV-responsive element.

Identification of protein complexes binding to the EBV-responsive element. EMSAs were performed to identify the nuclear protein complexes that bound to the EBV-responsive element. A DNA mobility shift pattern was observed with EBV$^+$ B-LCL nuclear extracts incubated with a labeled DNA probe spanning positions −1181 to −1053, which includes the EBV-responsive region. A diffuse set of bands (upper arrow-

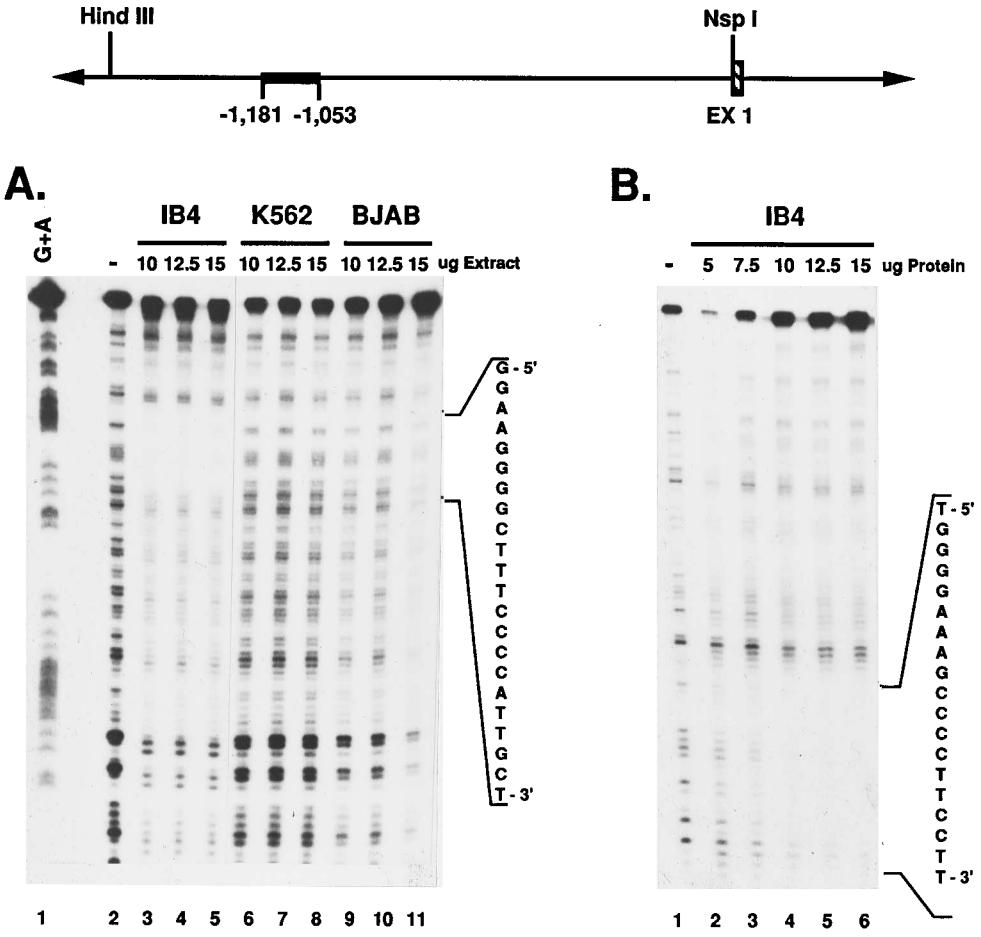

5' --GGAA**GGGGCTTTCC**CCATTGCT 3'
3' TTCCTT**CCCCGAAAGG**GGT----- 5'

FIG. 4. Identification of an NF-κB DNA binding motif within the EBV-responsive element by DNase I protection assay. The structure of the CD48 genomic DNA fragment is shown; the thick bar indicates the boundaries of the DNase I footprinting probes which were incubated with crude nuclear protein extracts from EBV^+ or EBV^- cell lines. Ex 1, exon 1. The number above each lane indicates the amount of protein extract added to the binding reaction (in micrograms). (A) Demonstration of a specific footprint with EBV^+ but not EBV^- nuclear extracts. The protected region was determined by reference to a G+A Maxam-Gilbert ladder, resolved in parallel (lane 1), and is bracketed at the right, with the 5′ and 3′ orientation noted. (B) EBV^+ IB4-LCL nuclear extracts protect the identical sequence (bracketed at the right) on the complementary strand. Protected regions identified in panels A and B are aligned below, with the NF-κB site shown in boldface.

head) and two tightly resolved bands (middle and lower arrowheads) were detected (Fig. 6, lanes 1 and 2). The middle band was not detected with EBV^- nuclear extracts (lanes 3 to 5), even when 10-fold more nuclear extract was added to the EMSA. The protein-DNA complexes (middle and lower arrowheads) were specific since they were efficiently competed for with a 25- to 200-fold molar excess of unlabeled target DNA (lanes 7 to 10) but not with unrelated binding sites (EBNA-1; lanes 11 to 14; Oct-1, not shown). If the putative NF-κB site was mutated, the specific protein-DNA complexes were no longer detected (Fig. 7A; compare lane 2 with lane 1), nor could unlabeled, mutated DNA compete with the wild-type probe for binding of the complexes when added at a 100-fold molar excess (not shown). A second band (lower arrowhead) was also detected with EBV^+ B-LCLs nuclear extracts (Fig. 6, lanes 1 and 2; Fig. 7, lane 1). This lower band could not be considered specific since (i) it was also detected with EBV^- nuclear extracts (Fig. 6, lanes 3 to 5; Fig. 7A, lane 3) and (ii) it was inefficiently competed for with a 25- to 200-fold molar excess of the corresponding unlabeled DNA fragment (Fig. 6, lanes 7 to 10). We conclude, therefore, that a specific nuclear protein complex, found in EBV^+ B-LCLs, binds to the EBV-responsive element and that the putative NF-κB site is essential for binding of the complex.

Competitive EMSA analysis. Competitive EMSA analysis was performed with a known NF-κB DNA binding motif as an initial test of whether NF-κB/Rel factors are components of the nuclear protein-DNA complexes detected with EBV^+ B-LCLs. As shown (Fig. 7B, lanes 4 and 5), competition with a 50- or 100-fold molar excess of an unlabeled 34-bp oligonucleotide, containing the human Igκ light-chain NF-κB consensus sequence (lanes 4 and 5), prevented formation of both the

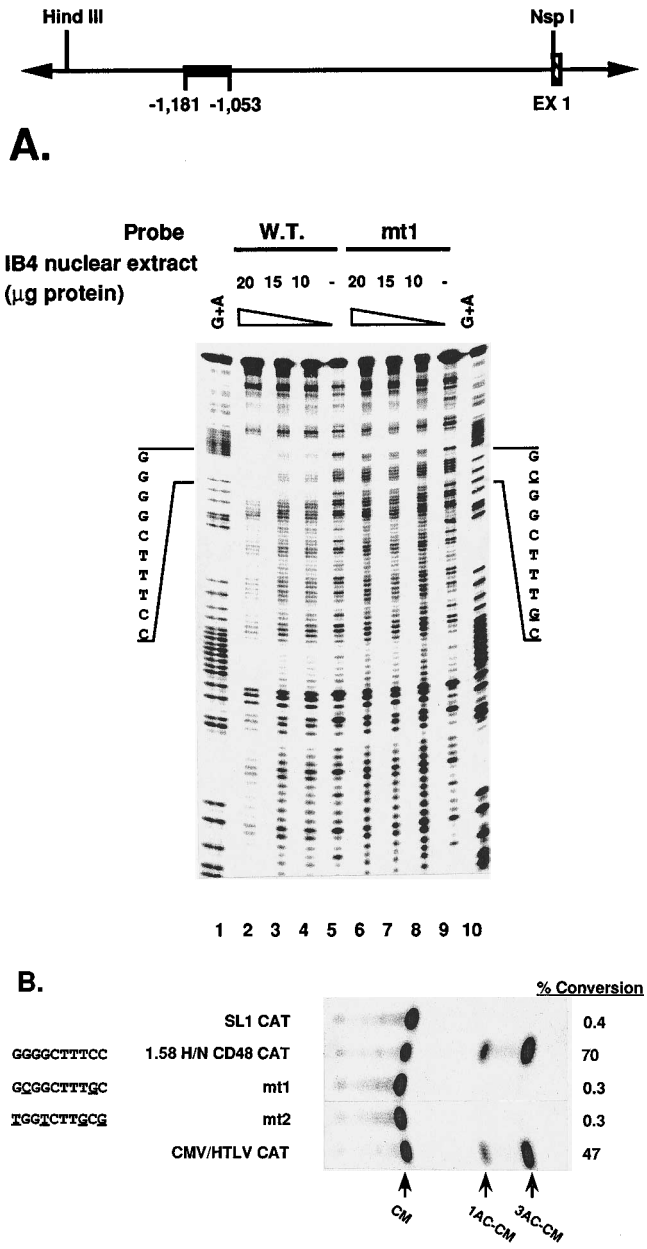

FIG. 5. Mutational analysis of the NF-κB site within the EBV-responsive element. The structure of the CD48 genomic DNA fragment is shown; the thick bar indicates the boundaries of the DNase I footprinting probe. Ex 1, exon 1. (A) DNase I footprinting analysis of CD48 sequences containing either a wild-type (W.T.; lanes 2 to 5) or mutated (mt1; lanes 6 to 9) NF-κB site within the EBV-responsive element (results displayed for IB4 nuclear extracts). The protected region was determined by reference to a G+A Maxam-Gilbert ladder, resolved in parallel (lanes 1 [wild-type G+A] and 10 [mutant G+A]). The protected region is indicated at the left for the wild-type sequence, while the unprotected mutated sequence is bracketed at the right. Mutated nucleotides are underlined. (B) Transcriptional activity in IB4 of −1.58 CAT reporter gene constructs containing either a wild-type or mutated NF-κB site within the EBV-responsive element. The sequences of the wild-type and mutated (mt1 and mt2) NF-κB sites are indicated, with mutated nucleotides underlined.

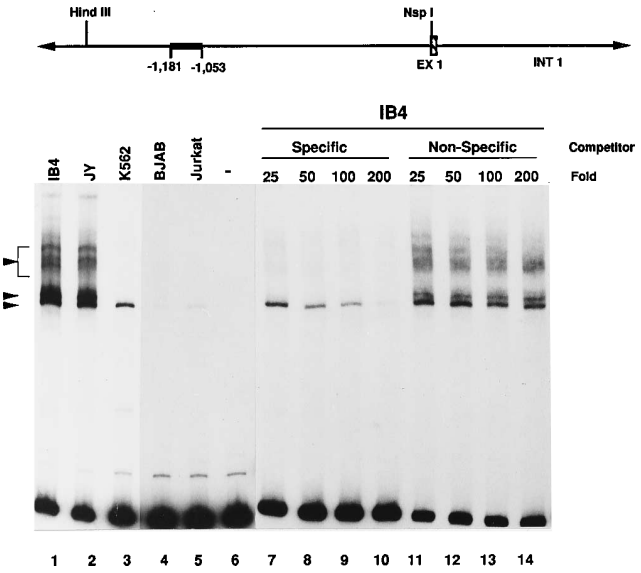

FIG. 6. Specific protein-DNA interactions within the EBV-responsive sequences detected by EMSA. The structure of the CD48 genomic DNA fragment is shown at the top; the thick bar indicates the boundaries of the EMSA probe. Ex 1, exon 1; INT 1, intron 1. This DNA probe was incubated with crude nuclear proteins from EBV$^+$ or EBV$^-$ cell lines and subjected to EMSA (lane 6, no extract control). Upper and middle arrowheads denote EBV-specific complexes. The lower arrowhead denotes a nonspecific complex shifted with all extracts. For binding reactions which include competitors (lanes 7 to 14), the fold molar excess is shown above each lane. In this experiment, unlabeled probe was the specific competitor and the EBNA-1 binding site was the nonspecific competitor.

middle and upper broad complex of bands. Again, the lower nonspecific band was not affected. Unlabeled probe, used as a specific competitor DNA (lanes 2 and 3), or an oligonucleotide containing the mouse Igκ light-chain NF-κB consensus site (not shown) also competed efficiently for binding to the putative NF-κB site, while an oligonucleotide with a mutated Igκ NF-κB site failed to compete for binding (lane 6). These findings suggest that NF-κB-related proteins bind to the EBV-responsive element.

NF-κB1 (p50) is a component of the middle nuclear protein complex. Supershifting antisera, raised against several NF-κB/Rel family proteins, were included in the EMSA binding reaction to identify which protein subunits are present in the specific complexes. We were able to directly demonstrate the presence of the NF-κB1 (p50) protein subunit in these complexes with two independently raised antisera (Fig. 7C, lanes 1 and 3). Compared with preimmune sera (lane 2), the immune antisera clearly supershifted the entire middle complex and altered the mobility of the diffuse upper bands as well. Therefore, one of the specific nuclear proteins that binds to the EBV-responsive element is NF-κB1 (p50). Antisera directed against epitopes of the RelA (p65) or c-*rel* family members did not affect the apparent mobility of the middle complex (not shown), suggesting that it may be a p50 homodimer. However, we do have preliminary evidence to suggest that components of the upper diffuse bands are shifted with these antisera.

Function of the EBV-inducible element in EBV$^-$ B-cell tumor lines before and after conversion with EBV. The CD48 gene is active in lymphoid lines, irrespective of their EBV status. The deletion analysis demonstrated that this reflected the action of different positive regulatory elements, an EBV-inducible element for EBV$^+$ B-LCLs and an unmapped element for the EBV$^-$ lymphoid tumor lines. It has been reported that infection of EBV$^-$ B-lymphoid tumor lines causes them to become more lymphoblastoid in phenotype (7, 9, 42). We wished to test if infection of these cells could drive them far

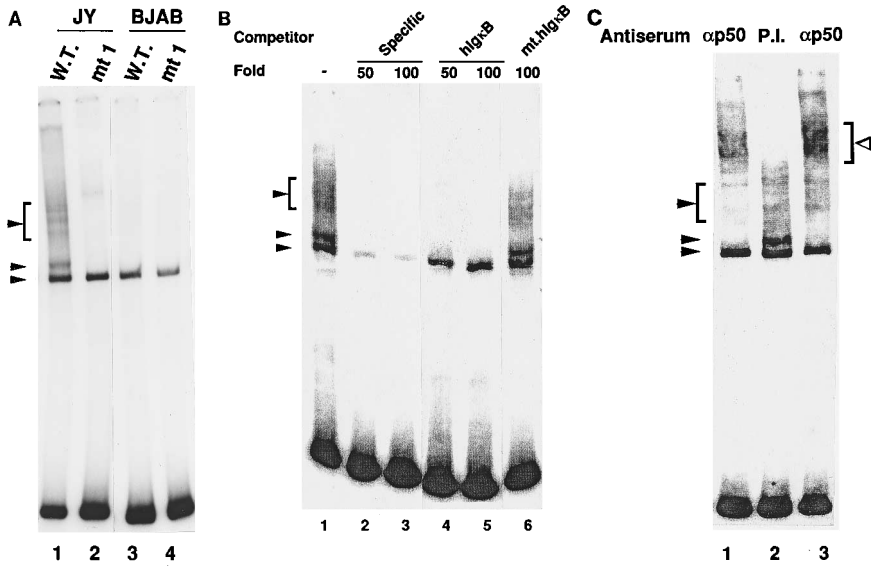

FIG. 7. EMSA analysis of the specific complexes binding to the EBV-responsive element. (A) EMSA comparing binding profiles of DNA probes containing either a wild-type or mutated NF-κB site within the EBV-responsive element. End-labeled DNA probes were incubated with crude nuclear proteins from the EBV$^+$ B-LCL JY (lanes 1 and 2) or the EBV$^-$ BJAB cell line (lanes 3 and 4) and subjected to native gel electrophoresis. The DNA probe used in the binding reaction, either wild type (W.T.) or mt1, is indicated above each lane. Upper and middle arrowheads denote EBV-specific complexes formed with the wild-type EMSA probe but not with the mutated probe. The lower arrowhead denotes a nonspecific complex shifted with all extracts. (B) NF-κB oligonucleotide competition experiment. An end-labeled DNA probe, spanning the EBV-responsive element (−1.181 to −1053), was incubated with EBV$^+$ B-LCL nuclear extracts (shown for IB4; lanes 1 to 6). Upper and middle arrowheads denote EBV-specific complexes which are competed for when unlabeled probe DNA (specific; lanes 2 and 3) or a 34-bp oligonucleotide containing a wild-type NF-κB binding site (human Igκ light-chain intronic κB site [hlgκB]; lanes 4 and 5) is added to the reaction but not when an oligonucleotide containing a mutated hIgκB site is added (lane 6). No competitor was added to lane 1. The lower arrowhead denotes a nonspecific complex shifted with all extracts. (C) Supershifting analysis of the protein-DNA complexes bound to the EBV-responsive element. Independently raised supershifting antisera (lanes 1 and 3), directed against different regions of the N terminus of NF-κB1 (p50), were added to the EMSA binding reaction mixtures containing IB4 nuclear extracts (described in the legend to Fig. 6). Upper and middle filled arrowheads denote complexes which are supershifted with specific antisera but not with preimmune sera (lane 2). The open arrowhead denotes the position of supershifted complexes. P.I., preimmune sera.

enough toward the lymphoblastoid phenotype to allow the EBV-responsive element to become active.

As shown in Fig. 8A, −1.58 CAT showed equivalent and low activities in BL41 and BJAB whether they were uninfected or infected with the laboratory strain B95-8, used to make the EBV$^+$ B-LCLs in Table 1. Furthermore, no difference in activity was seen between −869 CAT and −1.58 CAT in the B95-8-converted lines, indicating that the EBV-responsive element was not functional in these cell lines. This experiment demonstrates that infection of EBV$^-$ B-cell tumor lines does not drive them to become sufficiently lymphoblastoid in phenotype to allow the EBV-responsive element to function. We conclude, therefore, that EBV inducibility of the element is restricted to normal B cells.

NF-κB alone is insufficient to activate the element. The EBV-inducible element in the CD48 gene contains an essential NF-κB site, and EBV LMP-1 has been reported to activate NF-κB (18). We wished to confirm the latter observation in lymphoid cells and test if NF-κB alone was sufficient to activate the EBV-inducible element in the EBV$^-$ B-cell tumor lines.

A construct containing two copies of the CD48 NF-κB site cloned upstream of the TK CAT promoter (pCD48 NF-κB TK CAT) showed high activity in IB4 cells and low activity in BJAB cells (Fig. 8B). A control plasmid (mt NF-κB TK CAT), containing mutated NF-κB sites, was completely inactive in both cell lines. As expected, −1.58 CAT had no detectable activity in BJAB cells but was highly active in IB4 cells. Cotransfection of an LMP-1 expression vector (pSV2 BNLF1) into the BJAB cells had no effect on the −1.58 CAT construct but resulted in a marked transactivation, about 10-fold, of the pCD48 NF-κB TK CAT construct (Fig. 8B) and of other constructs containing NF-κB sites from the human or murine Igκ loci, the c-*myc* gene, or the human immunodeficiency virus long terminal repeat (not shown). The same results were obtained when NF-κB activity was induced directly, via expression vectors for the p50 and p65 components of NF-κB, or by phorbol myristate acetate induction (not shown). No transactivation by LMP-1, NF-κB, or phorbol myristate acetate was seen when the NF-κB sites were inactivated by specific mutation (for example, the mt NF-κB TK CAT construct) (not shown). These experiments demonstrate that LMP-1 can induce NF-κB activity in human B-lymphoid cells and that NF-κB, expressed directly or indirectly through LMP-1, can transactivate the CD48 NF-κB site. NF-κB alone, however, is not sufficient to activate the EBV-responsive element.

DISCUSSION

In this paper, we report on the identification and mapping of an EBV-responsive element within the upstream region of the CD48 gene. Furthermore, we have shown that the element binds a nuclear protein complex, only found in extracts from EBV$^+$ B-LCL, and that a functional NF-κB site is an essential component of the element. Since NF-κB is a classical mediator of gene regulation during B-cell activation, this observation confirms that EBV exploits physiologic pathways to alter the phenotype of resting mature B cells as it drives them to become proliferating lymphoblasts.

The CD48 promoter, localized between positions −234 and −110 upstream of exon 1, was only active in lymphoid cell lines. However, the promoter is negatively regulated in lym-

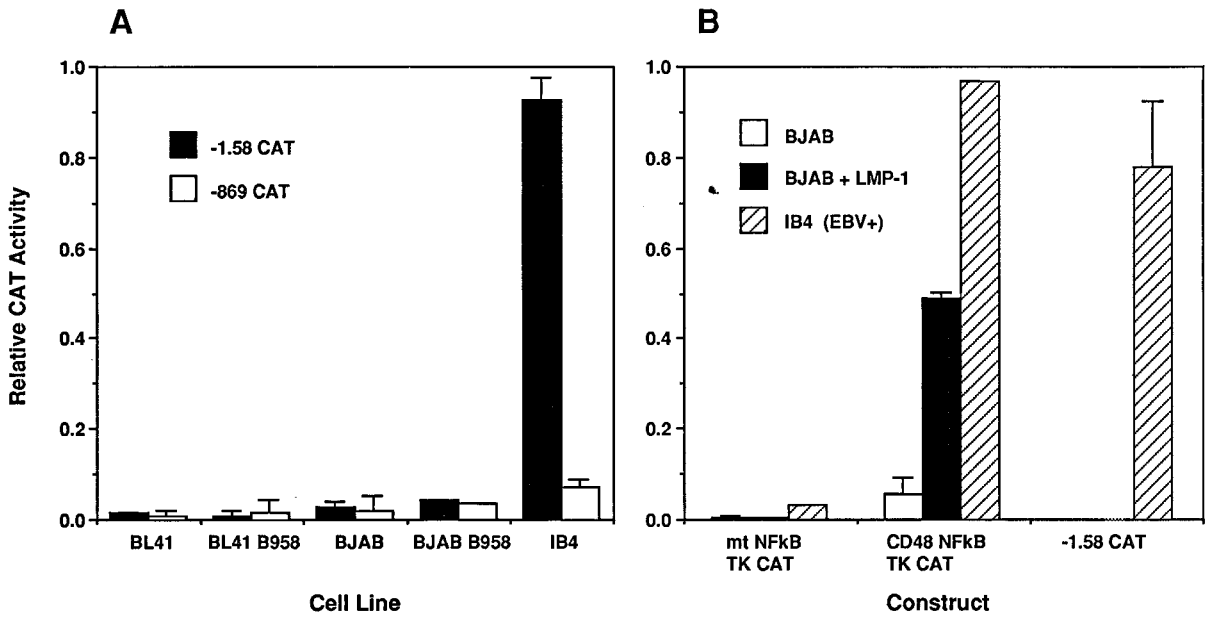

FIG. 8. (A) The EBV-responsive element does not function in in vitro-infected EBV$^-$ BL lines. The bar graph shows a quantitative comparison of relative CAT activities following transient transfection of −1.58 CAT or deletion construct −869 CAT into EBV$^-$ BL cell lines BL41 and BJAB before and after infection with the B95-8 strain of EBV. The EBV$^+$ B-LCL IB4 was included as a control to demonstrate the activity of the EBV-responsive element. The experiment was performed as described in the legend to Fig. 1. (B) EBV-encoded LMP-1 induces NF-κB but fails to transactivate −1.58 CAT. The bar graph shows a quantitative comparison of relative CAT activities following transient transfection of CAT reporter constructs consisting of either two CD48 NF-κB sites upstream of the TK promoter (pCD48 NF-κB TK CAT) or the same construct but with two mutated NF-κB sites (mt NF-κB TK CAT) or the −1.58 CAT construct. Each construct was transfected into the EBV$^-$ line BJAB in the presence or absence of an LMP-1 expression vector (pSV2 BNLF1) or into the EBV$^+$ B-LCL IB4 as a control. The experiment was performed as described in the legend to Fig. 2.

phoid lines by elements present further upstream, between −599 and −999. In order for the CD48 gene to be expressed, the transcriptional silencers need to be overridden, and the positive elements required for this activation are different in EBV$^+$ B-LCLs and EBV$^-$ lymphoid lines. The element required to restore activity in the EBV$^+$ B-LCLs was localized between positions −1245 and −1066. The sequences necessary to restore activity in the EBV$^-$ lymphoid lines have not been mapped since they are not present in the largest construct that we have tested, −1.58 CAT.

From these observations, we conclude that there are two distinct mechanisms for activating the CD48 gene, one for mature resting B cells, which is exploited by EBV, and another, exemplified by EBV$^-$ lymphoid tumor lines such as EBV$^-$ BL. This presumably reflects the fact that EBV$^-$ BL is a different cell type from the mature B cell that gives rise to the EBV$^+$ B-LCL. BLs are believed to derive from the germinal center centrocyte/centroblast and do not express the activated phenotype in vivo (27). When EBV$^-$ BL cell lines are infected with EBV in vitro, a tiny fraction of the cells become stably infected, and these cells tend to move toward a more activated/lymphoblastoid phenotype (7, 41, 42). There is a great deal of heterogeneity, between cell lines and between clones from the same BL line, in the degree to which individual markers are altered in their expression by EBV infection. It is apparent that genes activated by infection of mature resting B cells may be regulated differently upon infection of BL cells. This is most clearly demonstrated with CD48. CD48 is already expressed by EBV$^-$ B-cell lines through the action of an as yet unmapped element(s). EBV infection of these cells is not sufficient to activate the EBV-responsive element. However, we know that the EBV-responsive element functions in EBV$^+$ cells that are truly lymphoblastoid in phenotype, i.e., the EBV$^+$ B LCL. Therefore, we can conclude that EBV infection of EBV$^-$ B-cell tumor lines fails to push them to become sufficiently lymphoblastoid in character as to allow the activation of the EBV-responsive element. This means that the element is EBV responsive only upon infection of the natural target for EBV, the resting mature B cell.

NF-κB expressed directly or via LMP-1 can transactivate the CD48 NF-κB site when cotransfected into EBV$^-$ BLs. This finding suggests a role for LMP-1 and NF-κB in the regulation of CD48 by EBV, yet it is apparent that LMP-1 and NF-κB are not sufficient to transactivate the CD48 NF-κB site in the context of its flanking sequences. There is precedence for this in the literature, where several studies demonstrate that sequences surrounding the NF-κB site can influence the binding and/or function of NF-κB, for example, with the interleukin-2 receptor alpha chain (8), beta interferon (25), and ELAM-1 genes (44).

NF-κB belongs to a family of dimer-forming, *rel* oncogene-related proteins found in most cell types (reviewed in references 4 and 17). The nuclear protein complex in EBV$^+$ B-LCLs that binds to the EBV-responsive element of CD48 contains NF-κB1 p(50) probably as a homodimer. This was surprising, since the EBV-responsive element is positively transactivating and it is generally believed that p50 homodimers do not transactivate promoters (17). However, the other components of the complex are not yet clear. For example, we have noticed that the DNase I footprint also includes a perfect binding site for the Ets family member Pea-3 (AGG AAG) and have, on occasion, seen evidence for a second footprint, about 70 to 80 bp 3′ of the NF-κB site, that also includes a potential Ets binding site (see, for example, the 20-μg-loaded lane for the wild-type probe in Fig. 5A). How-

ever, to date we have been unable to demonstrate specific binding of Ets proteins to the EBV-responsive element.

NF-κB/Rel family members are expressed in the cytoplasm as inactive complexes in association with a member of the IκB family. Paradigmatically, signals emanating from the cell membrane lead to phosphorylation and dissociation of IκB from the complex, resulting in the migration of active NF-κB to the nucleus. It is not surprising therefore, that LMP-1 should be involved in activating NF-κB since LMP-1 is localized in the plasma membrane and, like NF-κB, is regulated in its activity by serine/threonine phosphorylation (32). LMP-1 is the only EBV latent protein clearly demonstrated to act as a dominant oncogene (2, 40) and is essential for the immortalization of normal, mature, resting B cells (20). It is inactivated by phosphorylation at threonine 324 and also has an extremely short half-life (2 to 3 h) (2, 30), being turned over by a specific proteolytic cleavage event that also inactivates the protein (31). It is possible that the same specific serine/threonine kinase phosphorylates NF-κB and LMP-1, leading to activation of NF-κB and inactivation of LMP-1, which would then be turned over through cleavage. The nature of the kinase, how LMP-1 activates it, and whether NF-κB is the only pathway of LMP-1 signaling remain to be ascertained.

In conclusion, the analysis presented here demonstrates that the CD48 gene is a good model for studying cellular genes that are differentially regulated by EBV in normal and EBV^- B-cell tumor lines. We are now attempting to better characterize the mechanism of signaling by LMP-1 and what other factors cooperate with LMP-1 to activate the CD48 gene in normal B cells. The CD48 NF-κB site is LMP-1/NF-κB inducible in EBV^- B-cell tumor lines, but the entire EBV-responsive element is not. By systematically adding back sequences to the CD48 NF-κB site, it should be possible to identify the DNA sequences that confer this unresponsiveness. Identification of these sequences should allow us to distinguish whether unresponsiveness in the EBV^- B-cell tumor lines is due to the presence of negatively regulating factors or the absence of positively regulating factors. Similarly, the CD48 NF-κB site does not bind nucleoprotein complexes that are specific to EBV^+ B-LCLs, whereas the entire EBV-responsive element does. By adding back sequences, it should also be possible to identify the elements required to impose EBV specificity on the CD48 NF-κB site. These sites may be the same as those that cause unresponsiveness in the EBV^- B-cell tumor lines. Once these sites and factors are identified, it should be possible to proceed to reconstruct the entire functional EBV-responsive element in the EBV^- B-cell tumor lines.

ACKNOWLEDGMENTS

We gratefully thank Nancy Rice and Ulrich Siebenlist for providing antisera, Emily Miyashita for assistance in preparation of deletion plasmids, and Gerry Parker for photographic expertise. We also thank Ananda Roy, Scott Brodeur, and Marlene Klaman for critical comments and suggestions.

This work was supported by Public Health Service grants AI 18757 and CA 31893 from the National Institutes of Health.

REFERENCES

1. **Abmayer, S., and J. L. Workman.** 1991. Preparation of nuclear and cytoplasmic extracts from mammalian cells, p. 12.1.1–12.1.7. *In* F. M. Ausubel, R. Brent, R. E. Kingston, D. D. Moore, J. G. Seidman, J. A. Smith, and K. Struhl (ed.), Current protocols in molecular biology, vol. 2. John Wiley & Sons, New York.
2. **Baichwal, V. R., and B. Sugden.** 1988. Transformation of Balb 3T3 cells by the BNLF1 gene of Epstein-Barr virus. Oncogene **2:**461–467.
3. **Baltimore, D., and R. Sen.** 1986. Inducibility of κ immunoglobulin enhancer-binding protein NF-κB by a posttranslational mechanism. Cell **47:**921–928.
4. **Bours, V., G. Franzoso, K. Brown, S. Park, V. Azarenko, M. Tomita-Yamaguchi, K. Kelly, and U. Siebenlist.** 1992. Lymphocyte activation and the family of NF-kappa B transcription factor complexes. Curr. Top. Microbiol. Immunol. **182:**411–420.
5. **Cann, A. J., Y. Koyanagi, and I. S. Y. Chen.** 1988. High efficiency transfection of primary human lymphocytes and studies of gene expression. Oncogene **3:**123–128.
6. **Clark, E. A., and P. J. Lane.** 1991. Regulation of human B-cell activation and adhesion. Annu. Rev. Immunol. **9:**97–127.
7. **Cordier, M., A. Calender, M. Billaud, U. Zimber, G. Rousselet, O. Pavlish, J. Banchereau, T. Tursz, G. W. Bornkamm, and G. M. Lenoir.** 1990. Stable transfection of Epstein-Barr virus (EBV) nuclear antigen 2 in lymphoma cells containing the EBV P3HR1 genome induces expression of B-cell activation molecules CD21 and CD23. J. Virol. **64:**1002–1013.
8. **Cross, S. L., N. F. Halden, M. J. Lenardo, and W. J. Leonard.** 1989. Functionally distinct NF-κB binding sites in the immunoglobulin κ and IL-2 receptor α chain genes. Science **244:**466–469.
9. **Dugas, B., J. F. Delfraissy, A. Calenda, M. Peuchmaur, C. Wallon, M. T. Rannou, and P. Galanaud.** 1988. Activation and infection of B-cells by Epstein-Barr virus. Role of calcium mobilization and of protein kinase C translocation. J. Immunol. **141:**4344–4351.
10. **Duyao, M. P., D. J. Kessler, D. B. Spicer, C. Bartholomew, J. C. Cleveland, M. Siekevitz, and G. E. Sonenshein.** 1992. Transactivation of the c-*myc* promoter by human T cell leukemia virus type 1 tax is mediated by NFκB. J. Biol. Chem. **267:**16288–16291.
11. **Epstein, M. A., and B. G. Achong (ed.).** 1986. The Epstein-Barr virus: recent advances. Wiley Medical Publications, New York.
12. **Faisst, S., and S. Meyer.** 1992. Compilation of vertebrate-encoded transcription factors. Nucleic Acids Res. **20:**3–26.
13. **Fisher, R. C., and D. A. Thorley-Lawson.** 1991. Characterization of the Epstein-Barr virus-inducible gene encoding the human leukocyte adhesion and activation antigen Blast-1 (CD48). Mol. Cell. Biol. **11:**1614–1623.
14. **Fisher, R. C., and D. A. Thorley-Lawson.** 1993. Unpublished data.
15. **Gorman, C. M., L. F. Moffat, and B. H. Howard.** 1982. Recombinant genomes which express chloramphenicol acetyltransferase in mammalian cells. Mol. Cell. Biol. **2:**1044–1051.
16. **Graham, F. L., and A. J. van der Eb.** 1973. A new technique for the assay of infectivity of human adenovirus 5 DNA. Virology **52:**456–467.
17. **Grilli, M., J. J. Chiu, and M. J. Lenardo.** 1993. NF-kappa B and Rel: participants in a multiform transcriptional regulatory system. Int. Rev. Cytol. **143:**1–62.
18. **Hammarskjold, M. L., and M. C. Simurda.** 1992. Epstein-Barr virus latent membrane protein transactivates the human immunodeficiency virus type 1 long terminal repeat through induction of NF-κB activity. J. Virol. **66:**6496–6501.
19. **Hammerschmidt, W., and B. Sugden.** 1989. Genetic analysis of immortalizing functions of Epstein-Barr virus in human B lymphocytes. Nature (London) **340:**393–397.
20. **Kaye, K. M., K. M. Izumi, and E. Kieff.** 1993. Epstein-Barr virus latent membrane protein 1 is essential for B-lymphocyte growth transformation. Proc. Natl. Acad. Sci. USA **90:**9150–9154.
21. **Kintner, C., and B. Sugden.** 1981. Identification of antigenic determinants unique to the surfaces of cells transformed by Epstein-Barr virus. Nature (London) **294:**458–460.
22. **Lacy, J., and H. Rudnick.** 1992. Transcriptional regulation of the human IgE receptor (FcεRII/CD23) by EBV: identification of EBV-responsive regulatory elements in intron 1. J. Immunol. **148:**1554–1560.
23. **Lane, P. J., J. A. Ledbetter, F. M. McConnell, K. Draves, J. Deans, G. L. Schieven, and E. A. Clark.** 1991. The role of tyrosine phosphorylation in signal transduction through surface Ig in human B-cells: inhibition of tyrosine phosphorylation prevents intracellular calcium release. J. Immunol. **146:**715–722.
24. **Lane, P. J., M. A. Valentine, T. Barret, F. McConnell, K. E. Meier, and E. A. Clark.** 1990. Surface molecules and signal transduction events in human B cells, p. 117–143. *In* J. C. Cambier (ed.), Ligands, receptors, and signal transduction in regulation of lymphocyte function. American Society for Microbiology, Washington, D.C.
25. **Lenardo, M. J., C. M. Fan, T. Maniatis, and D. Baltimore.** 1989. The involvement of NF-κB in β-interferon gene regulation reveals its role as a widely inducible mediator of signal transduction. Cell **57:**287–294.
26. **Ling, P. D., J. J. Hsieh, I. K. Ruf, D. R. Rawlins, and S. D. Hayward.** 1994. EBNA-2 upregulation of Epstein-Barr virus latency promoters and the cellular CD23 promoter utilizes a common targeting intermediate, CBF-1. J. Virol. **68:**5375–5383.
27. **MacLennan, I. C. M., Y. L. Liu, and N. R. Ling.** 1988. B-cell proliferation in follicles, germinal centre formation and the site of neoplastic transformation in Burkitt's lymphoma. Curr. Top. Microbiol. Immunol. **141:**138–148.
28. **Maxam, A. M., and W. Gilbert.** 1980. Sequencing end-labeled DNA with base-specific chemical cleavages. Methods Enzymol. **65:**499–560.
29. **Miller, G.** 1990. Epstein-Barr virus: biology, pathogenesis and medical aspects, p. 1921–1958. *In* B. N. Fields et al. (ed.), Virology, 2nd ed. Raven Press, New York.
30. **Moorthy, R., and D. A. Thorley-Lawson.** 1990. Processing of the Epstein-

Barr virus-encoded latent membrane protein p63/LMP. J. Virol. **64:**829–837.
31. **Moorthy, R. K., and D. A. Thorley-Lawson.** 1993. All three domains of the Epstein-Barr virus-encoded latent membrane protein (LMP-1) are required for transformation of Rat-1 fibroblasts. J. Virol. **67:**1638–1646.
32. **Moorthy, R. K., and D. A. Thorley-Lawson.** 1993. Biochemical, genetic, and functional analysis of the phosphorylation sites on the Epstein-Barr virus-encoded, oncogenic, latent membrane protein LMP-1. J. Virol. **67:**2637–2645.
33. **Pope, J. H.** 1979. Transformation by the virus *in vitro*, p. 205–223. *In* M. A. Epstein and B. G. Achong (ed.), The Epstein-Barr virus. Springer-Verlag, New York.
34. **Rosenthal, N.** 1987. Identification of regulatory elements of cloned genes with functional assays. Methods Enzymol. **152:**704–720.
35. **Thorley-Lawson, D. A., and C. Ianelli.** Unpublished data.
36. **Thorley-Lawson, D. A., and K. P. Mann.** 1985. Early events in Epstein-Barr virus infection provide a model for B-cell activation. J. Exp. Med. **162:**45–59.
37. **Thorley-Lawson, D. A., L. M. Nadler, A. K. Bhan, and R. T. Schooley.** 1985. Blast-2 (EBVCS), an early cell surface marker of human B-cell activation, is superinduced by Epstein-Barr virus. J. Immunol. **134:**3007–3012.
38. **Thorley-Lawson, D. A., R. T. Schooley, A. K. Bhan, and L. M. Nadler.** 1982. Epstein-Barr virus superinduces a new human B-cell differentiation antigen (B-last-1) expressed on transformed lymphoblasts. Cell **30:**415–425.
39. **Tompkinson, B., E. Robertson, and E. Kieff.** 1993. Epstein-Barr virus nuclear proteins EBNA-3A and EBNA-3C are essential for B-lymphocyte growth transformation. J. Virol. **67:**2014–2025.
40. **Wang, D., D. Liebowitz, and E. Kieff.** 1985. An EBV membrane protein expressed in immortalized lymphocytes transforms established rodent cells. Cell **43:**831–840.
41. **Wang, D., D. Liebowitz, F. Wang, C. Gregory, A. Rickinson, R. Larson, T. Springer, and E. Kieff.** 1988. Epstein-Barr virus latent membrane protein alters the human B-lymphocyte phenotype: deletion of the amino terminus abolishes activity. J. Virol. **62:**4173–4184.
42. **Wang, F., C. Gregory, C. Sample, M. Rowe, D. Liebowitz, R. Murray, A. Rickinson, and E. Kieff.** 1990. Epstein-Barr virus latent membrane protein (LMP1) and nuclear proteins 2 and 3C are effectors of phenotypic changes in B lymphocytes: EBNA-2 and LMP1 cooperatively induce CD23. J. Virol. **64:**2309–2318.
43. **Wang, F., H. Kikutani, S. Tsang, T. Kishimoto, and E. Kieff.** 1991. Epstein-Barr virus nuclear protein 2 transactivates a *cis*-acting CD23 DNA element. J. Virol. **65:**4101–4106.
44. **Whelan, J., P. Ghersa, R. Hooft van Huijsduijnen, J. Gray, G. Chandra, F. Talabot, and J. F. DeLamarter.** 1991. An NF-κB-like factor is essential but not sufficient for cytokine induction of endothelial leukocyte adhesion molecule 1 (ELAM-1) gene transcription. Nucleic Acids Res. **19:**2645–2653.
45. **Yokoyama, S., D. Staunton, R. Fisher, M. Amiot, J. Fortin, and D. A. Thorley-Lawson.** 1991. Expression of the Blast-1 activation/adhesion molecule and its identification as CD48. J. Immunol. **146:**2192–2200.